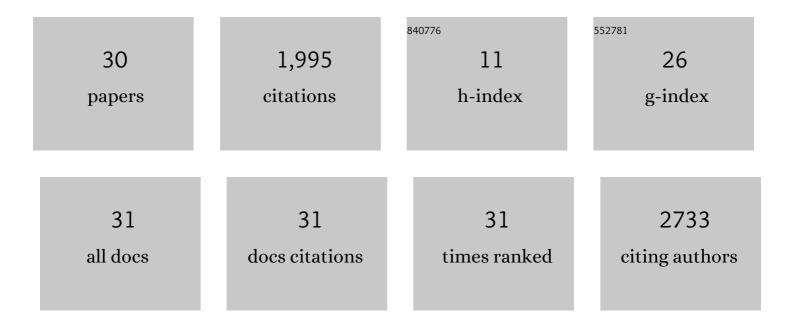
Yoshiteru Seo

List of Publications by Year in descending order

Source: https://exaly.com/author-pdf/2286827/publications.pdf Version: 2024-02-01



#	Article	IF	CITATIONS
1	Size-selective loosening of the blood-brain barrier in claudin-5–deficient mice. Journal of Cell Biology, 2003, 161, 653-660.	5.2	1,557
2	Multiquantum filters and order in tissues. NMR in Biomedicine, 2001, 14, 112-132.	2.8	139
3	Detection of hypothalamic activation by manganese ion contrasted T1-weighted magnetic resonance imaging in rats. Neuroscience Letters, 2002, 326, 101-104.	2.1	39
4	Proton double-quantum filtered MRI—A new method for imaging ordered tissues. Magnetic Resonance in Medicine, 1998, 40, 720-726.	3.0	36
5	1H double-quantum-filtered MR imaging as a new tool for assessment of healing of the ruptured Achilles tendon. Magnetic Resonance in Medicine, 1999, 42, 884-889.	3.0	24
6	A 1H-nuclear magnetic resonance study on lactate and intracellular pH in frog muscle The Japanese Journal of Physiology, 1983, 33, 721-731.	0.9	24
7	Sequence of forebrain activation induced by intraventricular injection of hypertonic NaCl detected by Mn2+ contrasted T1-weighted MRI. Autonomic Neuroscience: Basic and Clinical, 2004, 113, 43-54.	2.8	22
8	Anisotropic and restricted diffusion of water in the sciatic nerve: A2H double-quantum-filtered NMR study. Magnetic Resonance in Medicine, 1999, 42, 461-466.	3.0	21
9	Magnetic resonance imaging analysis of water flow in the mantle cavity of live <i>Mytilus galloprovincialis</i> . Journal of Experimental Biology, 2014, 217, 2277-2287.	1.7	17
10	Water permeability of capillaries in the subfornical organ of rats determined by Gdâ€DTPA 2―enhanced 1 H magnetic resonance imaging. Journal of Physiology, 2002, 545, 217-228.	2.9	14
11	A portable infrared photoplethysmograph: heartbeat of <i>Mytilus galloprovincialis</i> analyzed by MRI and application to <i>Bathymodiolus septemdierum</i> . Biology Open, 2016, 5, 1752-1757.	1.2	14
12	Effects of pCO2 on the CSF Turnover Rate in Rats Monitored by Gd-DTPA Enhanced T1-Weighted Magnetic Resonance Imaging The Japanese Journal of Physiology, 2001, 51, 555-562.	0.9	11
13	Mnâ€bicine: A low affinity chelate for manganese ion enhanced MRI. Magnetic Resonance in Medicine, 2011, 65, 1005-1012.	3.0	10
14	Roles of AQP5/AQP5-G103D in carbamylcholine-induced volume decrease and in reduction of the activation energy for water transport by rat parotid acinar cells. Pflugers Archiv European Journal of Physiology, 2012, 464, 375-389.	2.8	10
15	Testing the constant-volume hypothesis by magnetic resonance imaging of the mussel heart in the Mytilus galloprovincialis. Journal of Experimental Biology, 2013, 217, 964-73.	1.7	10
16	31P-NMR study of dog submandibular gland in vivo and in vitro using the Topical Magnetic Resonance The Japanese Journal of Physiology, 1985, 35, 729-740.	0.9	10
17	Magnetic resonance imaging of the temporomandibular joint in the rat compared with low-powered light microscopy. Archives of Oral Biology, 2011, 56, 1382-1389.	1.8	8
18	Effects of Na+ depletion on fluid secretion and levels of phosphorus compounds as measured by 31P-NMR in perfused canine mandibular gland The Japanese Journal of Physiology, 1984, 34, 587-597.	0.9	8

YOSHITERU SEO

#	ARTICLE	IF	CITATIONS
19	Mnâ€citrate and Mnâ€HIDA: intermediateâ€affinity chelates for manganeseâ€enhanced MRI. Contrast Media and Molecular Imaging, 2013, 8, 140-146.	0.8	4
20	Accumulation and excretion of manganese ion in the kidney of the <i>Mytilus galloprovincialis</i> . Journal of Experimental Biology, 2018, 221, .	1.7	4
21	NMR Imaging of Rigid Biological Tissues. , 0, , 445-457.		3
22	Roles of Keber's valve and foot chamber for foot manipulation in the clam Nodularia douglasiae. Biology Open, 2018, 8, .	1.2	3
23	Structure and Size-selective Permeability of the Synovial Membrane of the Temporomandibular Joint of the Mouse Measured by MR Imaging at 7T. Magnetic Resonance in Medical Sciences, 2015, 14, 115-122.	2.0	2
24	Lateral diffusion of manganese in the rat brain determined by T1 relaxation time measured by 1H MRI. Journal of Physiological Sciences, 2011, 61, 259-266.	2.1	1
25	Size-selective filtration of the atrial wall estimated from the accumulation of tracers in the kidney of the mussel Mytilus galloprovincialis. Journal of Experimental Biology, 2019, 222, .	1.7	1
26	Rat mandibular condyle and fossa grew separately then unified as a single joint at 20 days old, which was the weaning age. Journal of Oral Science, 2020, 62, 197-201.	1.7	1
27	In vivo 31P-NMR studies on aerobic recovery of frog muscle following tetanus The Japanese Journal of Physiology, 1984, 34, 927-931.	0.9	1
28	Cardiac function of the deep-sea bivalve, Calyptogena okutanii, observed at atmospheric pressure via magnetic resonance imaging. Deep-Sea Research Part I: Oceanographic Research Papers, 2022, 186, 103826.	1.4	1
29	Fast MR Imaging of Esophageal Motility. , 0, , 395-401.		Ο
30	The kidney of the <i>Nodularia</i> freshwater mussel has a larger filtration-size and counter-current system with improved water excretion compared with the seawater mussel <i>Mytilus</i> . Biology Open, 2021, 10, .	1.2	0